PHYSICAL REVIEW C **76**, 021603(R) (2007)

Single and double proton emissions from the $^{14}O + {}^{4}He$ interaction

Changbo Fu,[1] V. Z. Goldberg,[1,*] A. M. Mukhamedzhanov,[1] G. G. Chubarian,[1] G. V. Rogachev,[2] B. Skorodumov,[3] M. McCleskey,[1] Y. Zhai,[1] T. Al-Abdullah,[1] G. Tabacaru,[1] L. Trache,[1] and R. E. Tribble[1]

[1]*Cyclotron Institute, Texas A&M University, College Station, Texas 77843, USA*

[2]*Department of Physics, Florida State University, Tallahassee, Florida 32306, USA*

[3]*Department of Physics, University of Notre Dame, Indiana 46556, USA*

(Received 9 January 2007; published 15 August 2007)

We observed single and double proton emissions in the $^{14}O + {}^{4}He$ interaction by the thick target inverse kinematic (TTIK) method at initial energy for ^{14}O at 32.7 MeV. We found that the protons mainly originate from the resonance excitation of states in ^{18}Ne. The observed states in ^{18}Ne decay by protons mainly to proton unstable states in ^{17}F. It was found that the decay of a state in ^{18}Ne at $E_{ex} = 8.45$ MeV demonstrates the features of a decay by a correlated proton pair. The observed properties of the $^{14}O + {}^{4}He$ interaction make a previous interpretation for the rate of $^{14}O(^{4}He, p)^{17}F$ at astrophysical energies suspect. We show how the TTIK method should be modified to obtain the data of astrophysical interest.

DOI: 10.1103/PhysRevC.76.021603 PACS number(s): 23.50.+z, 24.30.Gd, 24.50.+g, 26.30.+k

Reactions between unstable nuclei and helium influence a variety of astrophysical processes [1]. They are important as link reactions between the nuclei in the *pp* chains and the CNO nuclei. They are important in violent stellar explosions, such as novae and x-ray bursts, and in the last stages of a supernova explosion, the so called α rich freeze-out [2]. However, the data on reaction rates between unstable nuclei and helium are scant because of experimental difficulties of the measurements (see, for example, Ref. [3]).

Recently, a RIKEN group [4] used the thick target inverse kinematics method (TTIK) [5] to make direct measurements of the $^{14}O(\alpha, p)^{17}F$ reaction for the first time. Their goal was to provide data to determine the role of this reaction in the ignition of the high temperature rp-process for x-ray bursts in neutron stars. (For the results of indirect measurements, see Ref. [6] and references therein.) Here we show that the main assumption made in Ref. [4], that the $^{14}O(\alpha, p)^{17}F$ reaction dominates in the production of low energy protons, is not justified. Rather the $\alpha + {}^{14}O$ interaction results in many strong resonances at energies above the energy region important to stellar processes, which mainly decay by protons to particle unstable states in ^{17}F. These protons together with those from the subsequent decays from ^{17}F create background that is much larger than the yield related to the $^{14}O(\alpha, p)^{17}F$ reaction in the astrophysically important energy region. To show this we used the TTIK method for the first time to study a reaction with three particles in the final state. We present a modification of the TTIK method that is needed to obtain the astrophysical information for (α, p) reactions under these conditions.

In the conventional TTIK technique [5], the beam is slowed down and stopped in the target while the light reaction products escape from the region of the interaction and are detected. The advantage of the TTIK method is that an excitation function can be measured in a large interval with a "single" beam energy. However, in this approach, the energy of the incident ion at the moment of the interaction is not fixed by the experimental conditions. Therefore it is impossible to interpret the spectra (i.e., to reconstruct the kinematics) without additional assumptions, even in the case of a two particle final state. For the data in Ref. [4], the authors assumed that the decay of $^{18}Ne^{*}$ went primarily to the ground and the first excited state of ^{17}F.

Here we report on studies of the $^{14}O + \alpha$ interaction by measuring the coincident $2p$ events. The initial energy of ^{14}O was small enough to guarantee that $^{16}O_{g.s.} + 2p$ was the only possible final state.

The experiment was carried out at the Texas A&M University Cyclotron Institute with the experimental setup shown in Fig. 1. A radioactive ^{14}O secondary beam with a central energy of 66 MeV, an intensity of 2×10^{5} pps, and a purity of about 99% was obtained with MARS [7] as described in Ref. [8]. The beam passed through two scintillator foils (BC-400) with thicknesses of 21 and 14 μm that were positioned before the entrance to the scattering chamber. The light signal from the particles passing through the foils was detected by two pairs of photomultiplier tubes (PMTs). The signals from the PMTs were used to monitor the beam, to obtain a "start" signal for time of flight (TOF) measurements, and to identify the main beam contamination, ^{7}Be, which has the same q/m as ^{14}O and could not be separated by the velocity filter of MARS. Because the Coulomb barrier is smaller for $^{7}Be + \alpha$ than for $^{14}O + \alpha$, the cross section of the reaction $^{7}Be(\alpha, p)^{10}B$ [9] at low energies could be up to 10^{3} times larger than that for the $^{14}O(\alpha, p)^{17}F$ reaction. Amplitude analysis of the PMT signals reduced the $^{7}Be/^{14}O$ ratio to the 10^{-4} level.

The scattering chamber was filled with ^{4}He (99.99% pure) up to a pressure of 0.85 atm and was separated from the high vacuum of MARS by a 3 μm Havar foil. The initial ^{14}O beam energy in the chamber was 32.7 MeV after the Havar foil.

The reaction products were observed by a detector array that was composed of four quadrant-silicon detectors (QSDs). They were mounted on a plane 90° to the beam axis and 295 mm from the entrance window. The coordinates of the QSDs' centers in the plane were $(x, y) = (\pm 42.5, \pm 37.5)$ mm.

*Corresponding author: goldberg@comp.tamu.edu

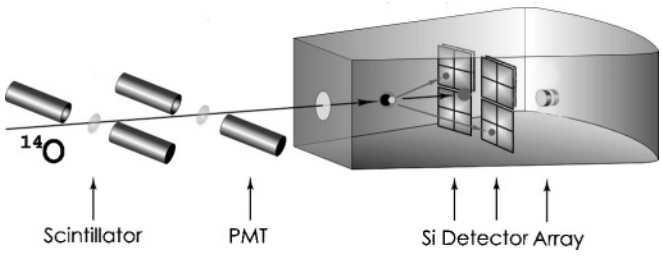

FIG. 1. The experimental setup that is described in the text.

Each QSD consisted of four square detectors (12.5 × 12.5 × 1 mm^3) and was followed by a large size veto detector to eliminate events that passed through the QSD. At a distance of 408 mm from the entrance window, a Si telescope of two round Si detectors (RSD) (15 mm in diameter × 1 mm thick) were placed at 0°. All silicon detectors were calibrated with a ^{228}Th α source and the resolution of each detector was better than 80 keV (FWHM).

Both energy and time signals from the detectors were recorded so that single events as well as coincidence events between any pair of detectors could be determined. The time resolution of the PMT-QSD was better than 3 ns, which was sufficient to separate protons and α particles, as shown below, and the time resolution of PMT-RSD was about 1 ns. More details of the experimental setup are given elsewhere [10].

A total of about 4800 $2p$ events was accumulated for the 2×10^{10} ^{14}O events. These events are shown in a Dalitz plot in Fig. 2(a). The concentration of events into spots is characteristic of sequential decays through intermediate states in ^{17}F. To show this more clearly, the data have been plotted in Fig. 2(b) with axes corresponding to excitation energy in ^{17}F. There is, of course, no *a priori* information that allows us to distinguish which one of the two coincident protons comes from the first step and which comes from the second step in the sequential decay process of $^{18}\mathrm{Ne}^* \rightarrow p + {}^{17}\mathrm{F}^* \rightarrow p + {}^{16}\mathrm{O} + p$. In generating Fig. 2(b), we translated both protons to an equivalent excitation energy in ^{17}F* using the proton energy and angle to account for the kinematics. Consequently, about 1/2 of the events are "correct" when projected to either axis. In Fig. 2(b), the positions of the spots, which correspond to decays through unbound states in ^{17}F, can be compared with known excitation energies in ^{17}F given in Fig. 3. The dominant intensity of events in Fig. 2 is distributed along lines that are parallel to the axes and correspond to known excitation energies of levels in ^{17}F at 3.10, 3.86, 4.64, and 5.22 MeV. Because the maximum energy of the incident ^{14}O particles is 32.7 MeV (≈7.3 MeV in c.m.), only a single final state, $^{16}\mathrm{O(g.s.)} + 2p$, was considered in calculating the excitation energies.

Figure 4 presents the excitation function for the process $^{14}\mathrm{O}(\alpha, 2p)^{16}\mathrm{O}$. It clearly shows that the process is dominated by resonances in ^{18}Ne in the region between 7.5 and 12.0 MeV. The 8.45 MeV level was observed before in the $^{16}\mathrm{O}(^3\mathrm{He}, n)$ reaction [11], and the 9.4 MeV level was likely observed in the $^{20}\mathrm{Ne}(p, t)$ reaction as a 9.2 MeV resonance in Ref. [11]. All other levels are observed here for the first time. No spin-parity assignments are known for the levels above 8 MeV in ^{18}Ne.

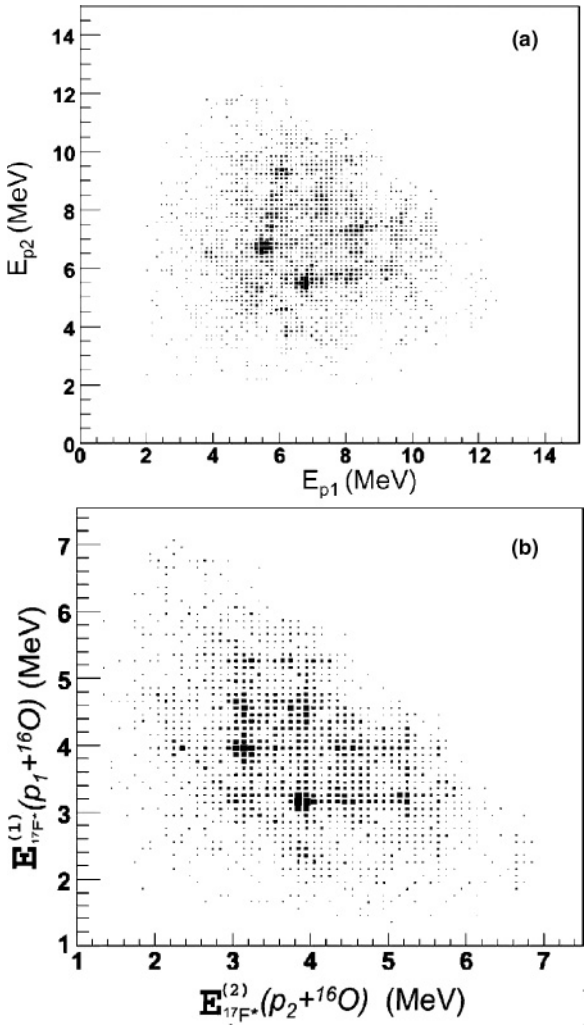

FIG. 2. Dalitz plots for the reaction $^{14}\mathrm{O}(\alpha, 2p)$. (A) Conventional Dalitz plot; (B) modified Dalitz plot with the coordinates shown as excitation energies in ^{17}F assuming a sequential $^{18}\mathrm{Ne}^* \rightarrow p_1 + {}^{17}\mathrm{F}^* \rightarrow p_1 + {}^{16}\mathrm{O} + p_2$ decay. $E^{(1)}_{^{17}F^*}$ is the excitation energy in ^{17}F based on the assumption that one proton of the coincident proton pair is from $^{18}\mathrm{Ne}^* \rightarrow p + {}^{17}\mathrm{F}^*$ and the other one is from $^{17}\mathrm{F}^* \rightarrow p + {}^{16}\mathrm{O}$. $E^{(2)}_{^{17}F^*}$ is the same with the role of the protons reversed.

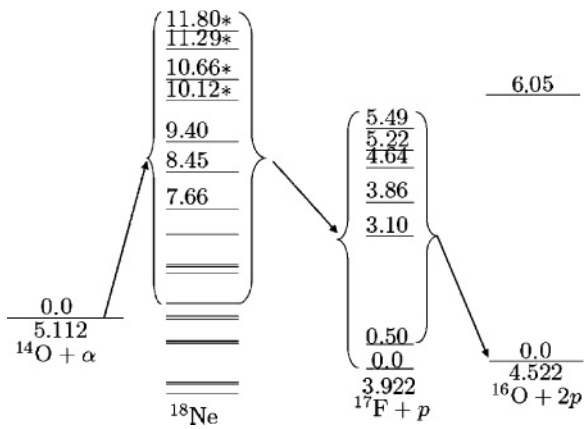

FIG. 3. Relevant ^{18}Ne and ^{17}F level scheme. Levels marked by * have not been seen before.

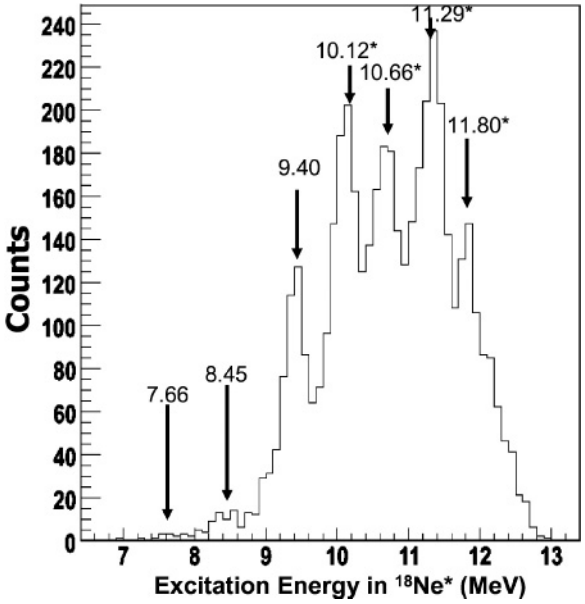

FIG. 4. The excitation function for the $^{14}O(\alpha, 2p)^{16}O$ reaction. Total cross section for 11.29 MeV level is estimated to be 50 mb. The energy resolution is about 0.2 MeV. Levels marked by * have not been seen before.

The proton decay of the ^{18}Ne*(8.45 MeV) level differed from the clearly sequential decay of other ^{18}Ne* states. To describe it, we calculated the two proton relative energy distributions for this decay using the Faddeev approach. The total $a \to 1 + 2 + 3$ decay amplitude is given by $R = R^{12} + R^{13} + R^{23}$, where R^{ij} is the Faddeev component that contains the final interaction between particles i and j of the three-body system $i + j + k$. In the case of ^{2}He decay, we should observe a peak in the energy spectrum of the R^{23} Faddeev's component due to the final state p-p interaction. It is given by $R^{23} = (R^{12} + R^{13})G_{23}^{(0)} f_{23}$, where $2 = p$ and $3 = p$, $G_{23}^{(0)}$ is the free Green's function of two protons, f_{23} is the half-off-energy shell (HOES) p-p scattering amplitude, taken as the sum of the HOES Coulomb scattering amplitude [12] plus the HOES Coulomb-modified nuclear p-p scattering amplitude calculated for the s-wave first rank Yamaguchi separable potential [13]. We replaced R^{12} and R^{13} by the Coulomb-centrifugal barrier penetration factor to obtain the results of the calculations that are compared with the experimental data in Fig. 5. In comparing the calculations to data, we took into account the angular acceptance of the particle detectors.

Because the orbital angular momentum of the resonance is not known, we calculated the p-p energy spectrum for relative orbital angular momenta ($l = 0 - 3$) of the ^{16}O core and the center of mass of two protons. The dotted line presents the results of the calculations when the dominant virtual p-p pole was eliminated. Noting that no parameters were fit besides the overall normalization, there is a good agreement between the experiment and calculations for the correlated $2p$ decay. Previously, diproton decay was suggested for the 6.15 MeV in ^{18}Ne [14], but this finding was questioned in Ref. [15]. The observation here suggests that the nuclear structure of ^{18}Ne* ($E_x = 8.45$ MeV) could be responsible for the correlated

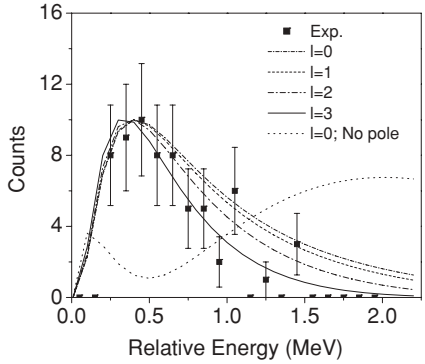

FIG. 5. The relative energy between two protons emitted from the 8.45 MeV level in ^{18}Ne*. The lines are for calculations described in the text.

pair decay, which manifests itself in the presence of the other possibilities for two body sequential decays. Additional experimental studies, including spin-parity assignments, for the 8.45 MeV level are needed to clarify this.

One result of the two proton coincidence study here is that a single proton spectrum will be a mixture of different processes. The same energy of protons can result from the process $^{18}\text{Ne}^* \to {}^{17}\text{F(g.s.)} + p^{(\text{g.s.})}$, or $^{18}\text{Ne}^* \to {}^{17}\text{F}^* + p^{(\text{ex})}$. The following idea was used to identify these processes experimentally [16]. Let the ^{14}O energy in the gas be 18 MeV, which corresponds to 4 MeV in the c.m. system. $E_{p^{(\text{g.s.})}}$ will be $\approx$9.5 MeV at 0° in the laboratory system. To produce the same energy for $p^{(\text{ex})}$, which corresponds to the ^{17}F* at 3.1 MeV, the ^{14}O energy should be about 28 MeV. This means that $p^{(\text{ex})}$ appears closer to the entrance window. Simple calculations show that the TOF difference between $p^{(\text{g.s.})}$ and $p^{(\text{ex})}$ is about 3 ns, where the TOF is started by the PMT and stopped by the Si detector at 0°. This difference is mainly defined by the time needed for an ^{14}O ion to slow down from an energy of 28 to 18 MeV in helium at a pressure of 0.85 atm. Thus, the proton from $^{17}\text{F}^*(>3.1\text{ MeV}) \to p + {}^{16}\text{O}$ could be separated from $p^{(\text{g.s.})}$.

Figure 6 shows this approach applied to data through a plot of the TOF versus the particle energy in the 0° detector. The banana at the top (slow moving particles) corresponds to the α particles from the $^{14}\text{O} + \alpha$ interaction. Below are the proton events corresponding to the population of the different states in ^{17}F. The banana corresponding to the population of the ground and the first excited state in ^{17}F is shown by the shadow. The parameters of the simulation code to calculate these lines were adjusted by using the 0° $2p$ coincidence data and the elastic α-particle data. Figure 7 shows a projection of the total proton yield at 0° from the $^{14}\text{O} + \alpha$ interaction onto the proton energy axis. (Coincidence events were used to specify the region of too "fast" events, which correspond to background from interactions of ^{14}O with the scintillation foils in front of the chamber.) The figure also shows the yield of protons from the $^{14}O(\alpha, p)$ reaction populating the particle stable states in ^{17}F. This yield (along the $p_0 + p_1$ shaded region) is evident at higher proton energies and is lost in the background at the lower energies when the energy of ^{14}O approaches the Coulomb barrier. The total proton

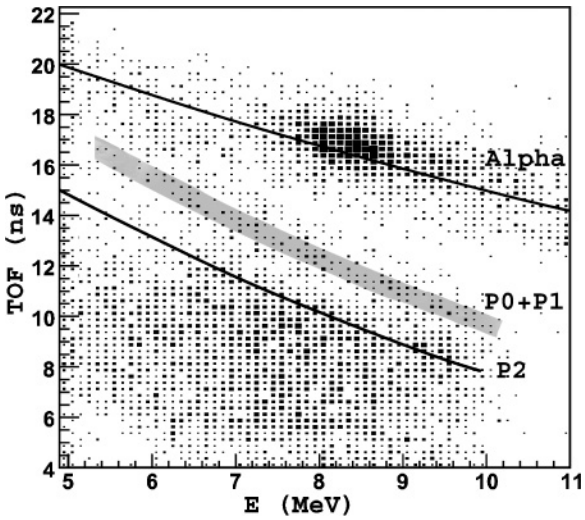

FIG. 6. The TOF-E spectrum of zero degrees.

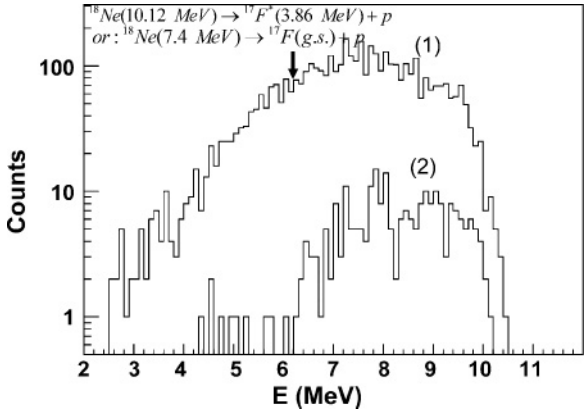

FIG. 7. Yield of protons at 0°. (1) Total proton yield; (2) yield of $p_0 + p_1$, see text for explanation.

yield rapidly decreases at low energy in agreement with the excitation function in Fig. 4. The arrow in Fig. 7 shows the energy (about 6 MeV) corresponding to the proton decay of the state at 10.12 MeV to the 3.86 MeV state in ^{17}F. If this proton energy is misassigned to a process populating the ground state in ^{17}F, then the calculated excitation energy in ^{18}Ne will be 7.4 MeV. This energy corresponds to the region of astrophysical interest. As can be seen in Fig. 6, the time resolution should be better to separate the $p_0 + p_1$ region for low-energy protons of astrophysical interest. The conditions used in the present experiment were optimized to observe p-p coincidences, and, therefore, the beam was stopped before the large PSD detectors. If instead the beam had been stopped after the PSDs but before the 0° detector by using lower pressure in the chamber, the separation between the proton regions would be about two times better due to the longer flight path of ^{14}O. Additionally there would be much better separation from α particles at low energies due to the lower energy loss of α's.

In summary, we measured the excitation function for the ^{4}He(^{14}O, $2p$) reaction, using the modified TTIK technique. We found that resonance excitation of levels in ^{18}Ne dominates this process. The dominant proton decay of these levels is to particle unstable states in ^{17}F. We also found that proton decay of the state at 8.45 MeV in ^{18}Ne demonstrates the properties of a decay by a correlated proton pair. The results above show that the method used here can be a powerful way to study the structure of proton rich nuclei. On the other hand, the results show that it is difficult to obtain data on the astrophysically important (α, p) reactions using the conventional TTIK method. These features were not previously known, and they may have led to an incorrect interpretation of the data in Ref. [4]. We also demonstrated that measurements of the TOF for protons in the TTIK method can be used to identify reactions occurring at different places in the gas target, thus making it possible to identify the process in question. Using this approach we could identify proton yield to particle stable states in ^{17}F in the ^{4}He(^{14}O, p) reaction.

The authors thank Dr. C. Gagliardi, Dr. S. Yennello, and Dr. R. Wada for their helpful advice and discussion of our study. This work was supported by the U.S. Department of Energy under Grants DE-FG02-93ER40773 and DE-FG52-06NA26207/A000 and was also partially supported by NSF Grant PHY-04-56463.

[1] A. E. Champagne and M. Wiesher, Annu. Rev. Nucl. Part. Sci. **42**, 39 (1992).
[2] A. F. Iyudin *et al.*, Nature (London) **396**, 142 (1998).
[3] A. A. Sonzogni *et al.*, Phys. Rev. Lett. **84**, 1651 (2000).
[4] M. Notani, S. Kubono, T. Teranishi *et al.*, Nucl. Phys. **A746**, 113c (2004); S. Kubono, T. Teranishi, M. Notani *et al.*, Eur. Phys. J. A **27**, Suppl. 1, 327 (2006).
[5] K. P. Artemov, M. S. Golovkov, V. Z. Goldberg *et al.*, Sov. J. Nucl. Phys. **52**, 480 (1990).
[6] B. Harss, J. P. Greene, D. Henderson *et al.*, Phys. Rev. Lett. **82**, 3964 (1999).
[7] R. E. Tribble, R. H. Burch, and C. A. Gagliardi, Nucl. Instrum. Methods A **285**, 441 (1989).
[8] V. Z. Goldberg, G. G. Chubarian, G. Tabacaru *et al.*, Phys. Rev. C **69**, 031302(R) (2004).
[9] J. C. Overley and W. Whaling, Phys. Rev. **128**, 315 (1962).
[10] C. Fu *et al.* (to be submitted).
[11] A. V. Nero, E. G. Adelberger, and F. S. Dietrich, Phys. Rev. C **24**, 1864 (1981).
[12] E. I. Dolinskii and A. M. Mukhamedzhanov, Sov. J. Nucl. Phys. **3**, 180 (1966).
[13] H. V. Heringen, Nucl. Phys. **A253**, 355 (1975).
[14] J. Gómez del Campo, A. Galindo-Uribarri, J. R. Beene *et al.*, Phys. Rev. Lett. **86**, 43 (2001).
[15] L. V. Grigorenko, R. C. Johnson, I. J. Thompson, and M. V. Zhukov, Phys. Rev. C **65**, 044612 (2002).
[16] A similar idea for a stable beam was used by G. V. Rogachev, Ph.D. thesis (Kurchatov Institute, Moscow, Russia, 1999).